*American Mineralogist, Volume 90, pages 1167–1176, 2005*

# The crystal-chemistry of holmquistites: Ferroholmquistite from Greenbushes (Western Australia) and hints for compositional constraints in $^{B}$Li amphiboles

**FERNANDO CÁMARA* AND ROBERTA OBERTI**

CNR-Istituto di Geoscienze e Georisorse, via Ferrata 1, I-27100 Pavia, Italy

## ABSTRACT

A systematic crystal-chemical investigation of orthorhombic holmquistites has been done to determine the reasons for their limited compositional variations. Structural constraints to the relative stability of $^{B}$Li amphiboles are also suggested by the occurrence of ferro- and ferri-ferroclinoholmquistites, and the lack of clinoholmquistite. Detailed crystal-chemical analysis shows: (1) a remarkable constancy in composition, both in terms of charge arrangement and of limited homovalent $^{M1,3}(Mg_{-1}Fe^{2+})$, $^{M2}(Al_{-1}Fe^{3+})$, and $^{O3}(OH_{-1}F)$ exchanges, (2) a remarkable constancy in the unit-cell dimensions, with the $Fe^{3+}$ content at the M2 site being the only factor affecting the *b* edge; (3) complete ordering of Li at the M4 site, in contrast with the common partitioning between the M4 and M3 sites in clinoamphiboles, which however couples with partial A-site occupancy; (4) complete ordering of trivalent cations at the M2 site; (5) an inverse relationship between the $Fe^{2+}$ and the $Fe^{3+}$ contents, which is interpreted as a way to keep the size of the octahedral strip constant; (6) a strong distortion of the octahedral sites, both in terms of angular variance and quadratic elongation.

$^{A}\square^{B}Li_2{}^{C}(Mg_3Al_2)^{T}Si_8O_{22}(OH)_2$ is the amphibole composition composed of the smallest possible structural moduli. Crystallization in *Pnma* symmetry, where the two double-chains of tetrahedra can assume different conformations, is probably required by the need to obtain a more suitable [5 + 1]-coordination for $^{B}$Li, and to shrink the cation-cation distances. This arrangement does not allow for extensive incorporation of larger homovalent substituents, which are hosted via mechanisms implying distortion of the octahedral sites.

During this work, a sample with $Fe^{2+}$ slightly but significantly higher than Mg was characterized, and then recognized as a mineral species by the IMA-CNMMN (2004-030). Holotype ferroholmquistite has $a = 18.287$ (1), $b = 17.680$ (1), and $c = 5.278$ (1) Å, and $V = 1706.6(1)$ Å$^3$. Its crystal-chemical formula is $^{A}K_{0.01}Na_{0.01}{}^{B}(Li_{1.88}Mg_{0.08}Na_{0.03}Fe^{2+}_{0.01})^{C}(Al_{1.89}Fe^{2+}_{1.70}Mg_{1.39}Mn^{2+}_{0.02})^{T}Si_{8.00}O_{22}(OH_{1.97}F_{0.03})$. Ferroholmquistite occurs as elongated black to bluish-violet prismatic crystals; it is biaxial negative, with $\alpha = 1.628$, $\beta = 1.646$, and $\gamma = 1.651$ ($\lambda = 589$ nm), $2V_x$ (calc.) = 55.1°. It is weakly pleochroic, with $\alpha$ = colorless, $\beta$ = pale violet-blue, and $\gamma$ = blue to deep violet; the calculated density is 3.145 g/cm$^3$. The holotype specimen belongs to the mineral collection of Renato and Adriana Pagano (Italy), and comes from the Greenbushes pegmatite (Western Australia). The analyzed sample has been deposited at the Museum of the Dipartimento di Scienze della Terra, Università di Pavia (Italy) under the code 2004-01.

## INTRODUCTION

The root name holmquistite defines a series of orthorhombic *Pnma* Group 1 amphiboles whose compositions can be expressed as $^{A}\square^{B}Li_2{}^{C}[(Mg,Fe^{2+})_3(Al,Fe^{3+})_2]^{T}Si_8O_{22}(OH)_2$. Holmquistites are rather rare amphiboles, and generally occur at the contact between lithium-rich pegmatites and country rocks; their formation has always been ascribed to metasomatism around highly fractionated lithium-rich pegmatites that intrude amphibolites (cf. London 1986 and Deer et al. 1997 for useful reviews). Notably, London (1986) first proposed that the occurrence of holmquistite might be used as a tool for pegmatite exploration.

The few available chemical analyses of holmquistites show a remarkable constancy in composition (see Deer et al. 1997 for a complete list). We re-calculated analyses nos. 10 and 14 based on more reasonable water contents and group-cation sums, compared all the data and noticed that (1) $^{T}$Al is always very low, (2) $^{C}$Al (+ very minor $Fe^{3+}$ and Ti contents) is always close to 2.0 atoms per formula unit (apfu), and (3) $^{C}$Mn, $^{B}$Ca, $^{B}$Na, and $^{A}$K are always very low or negligible. In particular, analysis no. 10 (from Alexander County, South Carolina; Palache et al. 1930) is the one most deviating from the ideal charge arrangement, having $^{T}$Al = 0.46, $^{B}$Ca = 0.19, and $^{A}$K = 0.13 apfu. Analysis no. 14 (from the Sayan Mountains, former USSR; Khvostova 1958), although suffering from analytical problems possibly implying overestimation of the Si and water contents, is the only one with $Fe^{2+} > Mg$.

Few structural and crystal-chemical data are available for holmquistite. Holmquistite from Mtoko (Zimbabwe) was studied by Whittaker (1969), Irusteta and Whittaker (1975), and Law and Whittaker (1981), who provided structure refinements, Mössbauer analysis, and IR spectroscopy. Although the original analysis

* E-mail: camara@crystal.unipv.it

(Knorring and Hornung 1961) was troublesome, possibly due to hornblende contamination, these authors concluded that Li is ordered at the M4 site, $Fe^{2+}$ at the M1 and M3 sites, and Al (with minor $Fe^{3+}$) is somewhat disordered between the M2, M1, and M3 sites. They also noted an unusual separation of the Mössbauer $Fe^{2+}$ doublets, and a strong $Fe^{2+}$ preference for the M3 site (0.52 apfu vs. 0.74 apfu at the 2 M1 sites). This scheme was later confirmed (except for the disorder of octahedral Al) by Walter et al. (1989) for a holmquistite crystal from Koralpe (Austria), and by Puvvada (1991) for two holmquistite samples (one from Greenbushes, Western Australia, and one from the QLC mine, Quebec). Litvin et al. (1973) provided a refinement of a holmquistite sample from Kola (Siberia), and suggested that the M4 cation is disordered off the twofold axis; however, their data are of poor quality (cf. the low number of unique reflections, 580, and the high *R* factor, 9%). Ishida (1990) reported IR data for one natural and one deuterated samples of holmquistite from Greenbushes (Western Australia). Complete Raman spectra and band assignment for holmquistite from the Martin Marietta quarry (North Carolina) were reported by Kloprogge et al. (2001).

Systematic investigations of monoclinic Li-bearing amphiboles based on structure refinements and complete (EMP + SIMS) in situ analyses have shown that Li occurs at the M3 site in sodic (Group 4) amphiboles, but partitions itself between the M4 and M3 sites in Group 1 and Group 5 amphiboles (cf. Oberti et al. 2003a, 2003b, 2004). They also showed that the holotype specimen of clinoholmquistite (Ginzburg 1965; Litvin et al. 1975) is actually fluoro-sodic-pedrizite, so that at present there is no evidence for the stability of the monoclinic structure in Fe-poor environments (Oberti et al. 2005). Therefore, there are at least two good reasons for a re-examination of the crystal-chemistry of holmquistite: (1) the need to understand the structural reasons for compositional constancy and cation order and (2) the identification of a structural limit, if any, which could determine a phase transition as a function of composition.

Holmquistite samples from the main known localities were gathered with the help of museum curators and several mineral collectors; a list of the investigated samples and their unit-cell parameters is provided in Table 1. The sample from the Greenbushes pegmatite (code 3380B in the Pagano's collection, sample 1 in this paper) is actually holotype ferroholmquistite (IMA-CNMMN 2004-030) and has been deposited at the Museum of the Dipartimento di Scienze della Terra, Università di Pavia, under the code 2004-01.

## Experimental methods and results

### X-ray analysis and structure refinement (SREF)

Holmquistite crystals were selected on the basis of optical and diffraction properties. Depending on their size, X-ray analysis and data collections were done either with a Philips PW-1100 four-circle diffractometer (crystals 3 and 7; Table 1) or with a Bruker AXS Smart APEX diffractometer (crystals 1, 2, 4, 5, and 6; Table 1) using graphite-monochromatized Mo$K\alpha$ X-radiation. Unit-cell dimensions for the crystals studied with the Philips PW-1100 diffractometer were calculated from least-squares refinement of the *d*-values obtained from 50 rows of the reciprocal lattice by measuring the center of gravity of each reflection and of the corresponding antireflection in the range $-30 < \theta < 30°$. Reflection profiles were integrated following the method of Lehmann and Larsen (1974) as modified by Blessing et al. (1974). Intensities were corrected for Lorentz-polarization and absorption following North et al. (1968). Unit-cell dimensions for the crystals studied with the Bruker AXS Smart APEX diffractometer were calculated from least-squares refinement of the angular positions of all the collected reflections. Three-dimensional data in the θ-range 3–35° were integrated and corrected for Lorentz, polarization, and background effects using the SAINT+ software version 6.02 (Bruker AXS). Raw intensities were corrected for absorption using the SADABS v. 2.03 program (Sheldrick 1996).

Full-matrix weighted least-squares refinements on $F^2$ were done using SHELXL-97 (Sheldrick 1997). The two independent hydrogen atoms were located by means of Fourier-difference maps after convergence of the least-squares procedure. They were added to the model, but their atom coordinates and isotropic displacement parameters were kept fixed during the final refinement cycles. Table 1 lists sample codes and selected crystal and refinement data, Table 2 lists atom coordinates, isotropic displacement parameters, and refined site-scattering values (ss, epfu), and Table 3 lists the geometric parameters relevant for the description of the crystal structure. Table 4[1] lists the anisotropic displacement parameters and Table 5[1] lists observed and calculated structure factors.

### Electron (EMP) and ion (SIMS) microprobe analysis

Complete chemical characterization was done for the same crystals used for the X-ray structure refinements. The crystals were embedded in epoxy, polished, and carbon coated. EMP analyses were done with a Cameca SX50 at the CNR-Istituto di Geologia Ambientale e Geoingegneria (IGAG), Rome. Analytical conditions were 15 kV accelerating voltage and 15 nA beam current, with a 5 μm beam diameter. The counting time was 20 s on both peak and background. Standards used were: wollastonite (Si$K\alpha$, TAP; Ca$K\alpha$, PET), periclase (Mg$K\alpha$, TAP), corundum (Al$K\alpha$ TAP), magnetite (Fe$K\alpha$, LIF), rutile (Ti$K\alpha$, LIF), and Mn metal (Mn$K\alpha$ LIF). Estimated analytical errors are 1% rel. for major elements and 5% rel. for trace elements. Data reduction was done with the PAP method (Pouchou and Pichoir 1985).

Samples were subsequently re-polished and gold-coated for SIMS analysis. Analysis of Li was done with a Cameca IMS 4f probe (CNR-IGG-PV, Italy) with a $^{16}O^-$ primary beam with diameter ~10 μm (corresponding to a beam current of ~4 nA). Secondary positive-ion currents were measured at masses 7 (Li) and 30 (Si, used as the reference element), and corrected for isotopic abundance. The accuracy of the $Li_2O$ measurements was shown to be around 10–15% rel. B, Be, and Cl ion signals, tested at 11, 9, and 37 mass numbers (amu), were negligible. Detailed analytical procedures are described by Ottolini and Oberti (2000). Crystal 4 (from Rwanda) was lost during re-polishing for gold-coating. Table 6 reports the complete chemical analyses and the resulting unit formulae calculated on the basis of 24 (O, OH, F) apfu when using the F and $H_2O$ contents from EMP analyses and from stoichiometry, respectively. The $Fe^{3+}$ content ($X\,Fe^{3+}$) was calculated based on overall charge balance with the constraint $^{T}Si \leq 8$ apfu. The calculated group-site scattering values (in electrons per formula unit, epfu) are also reported in Table 6; they are in good agreement with those obtained from structure refinement (Table 2).

[1]For a copy of Tables 4 and 5, Document AM-05-017 contact the Business Office of the Mineralogical Society of America (see inside cover of a recent issue for contact information). Deposit items may also be available on the American Mineralogist web site at http://www.minsocam.org.

**Table 1.** Samples, localities, and selected crystal and refinement data

| No.* | Locality | Code | *a* (Å) | *b* (Å) | *c* (Å) | *V* (Å³) | $R_{sym}$ % | $R_{all}$ % | w$R_{all}$ % | no. $F_{all}$ | θ-range |
|---|---|---|---|---|---|---|---|---|---|---|---|
| 1 | Greenbushes, W Australia | hph | 18.2872(6) | 17.6797(6) | 5.2784(1) | 1706.6(1) | 2.8 | 4.3 | 8.3 | 3854 | 2–35 |
| 2 | HS 119915, Siberia | inw | 18.277(2) | 17.650(1) | 5.2736(4) | 1701.1(2) | 5.0 | 6.2 | 13.1 | 3835 | 2–35 |
| 3 | Siberia | hxf | 18.277(1) | 17.646(1) | 5.2792(4) | 1702.7(2) | 4.4 | 8.7 | 8.0 | 2560 | 2–30 |
| 4 | Rwanda | ilm | 18.2754(7) | 17.6569(7) | 5.2738(2) | 1701.8(1) | 5.4 | 9.6 | 16.4 | 3841 | 2–35 |
| 5 | Zaire | imy | 18.3345(7) | 17.6955(7) | 5.2764(2) | 1711.9(1) | 4.4 | 4.6 | 10.4 | 3877 | 2–35 |
| 6 | Üto, Sweden | hpj | 18.335(1) | 17.693(1) | 5.2743(3) | 1711.0(2) | 3.8 | 9.8 | 19.3 | 3869 | 2–35 |
| 7 | Norway | hwn | 18.336(2) | 17.693(2) | 5.2755(6) | 1711.5(4) | 3.8 | 8.1 | 5.3 | 2580 | 2–30 |

* In order of decreasing site-scattering value at the (2M1+M3) sites.

**TABLE 2A.** Atom coordinates and displacement parameters ($U_{iso}$, Å$^2$) for the oxygen atoms

| Atom | | 1 | 2 | 3 | 4 | 5 | 6 | 7 |
|---|---|---|---|---|---|---|---|---|
| O1A | *x* | 0.1805(1) | 0.1804(1) | 0.1806(1) | 0.1806(2) | 0.1810(1) | 0.1812(2) | 0.1811(1) |
| | *y* | 0.1559(1) | 0.1563(1) | 0.1561(1) | 0.1566(2) | 0.1582(1) | 0.1585(2) | 0.1583(1) |
| | *z* | 0.0493(2) | 0.0494(3) | 0.0499(4) | 0.0496(6) | 0.0527(2) | 0.0525(6) | 0.0525(4) |
| | $U_{eq}$ | 0.006(1) | 0.006(1) | 0.007(1) | 0.007(1) | 0.008(1) | 0.006(1) | 0.007(1) |
| O1B | *x* | 0.0700(1) | 0.0701(1) | 0.0698(1) | 0.0701(2) | 0.0695(1) | 0.0694(2) | 0.0696(1) |
| | *y* | 0.1554(1) | 0.1556(1) | 0.1560(1) | 0.1560(2) | 0.1579(1) | 0.1577(2) | 0.1578(1) |
| | *z* | 0.7403(2) | 0.7396(4) | 0.7385(4) | 0.7402(6) | 0.7376(2) | 0.7375(6) | 0.7377(4) |
| | $U_{eq}$ | 0.006(1) | 0.007(1) | 0.007(1) | 0.006(1) | 0.008(1) | 0.005(1) | 0.006(1) |
| O2A | *x* | 0.1845(1) | 0.1844(1) | 0.1844(1) | 0.1845(2) | 0.1846(1) | 0.1848(2) | 0.1845(1) |
| | *y* | 0.0750(1) | 0.0753(1) | 0.0753(1) | 0.0756(2) | 0.0764(1) | 0.0764(2) | 0.0764(1) |
| | *z* | 0.5938(2) | 0.5931(4) | 0.5927(4) | 0.5922(6) | 0.5881(2) | 0.5878(6) | 0.5878(4) |
| | $U_{eq}$ | 0.006(1) | 0.006(1) | 0.008(1) | 0.006(1) | 0.008(1) | 0.006(1) | 0.006(1) |
| O2B | *x* | 0.0650(1) | 0.0652(1) | 0.0652(1) | 0.0651(2) | 0.0651(1) | 0.0646(2) | 0.0650(1) |
| | *y* | 0.0744(1) | 0.0746(1) | 0.0748(1) | 0.0747(2) | 0.0757(1) | 0.0756(2) | 0.0758(1) |
| | *z* | 0.1981(2) | 0.1968(3) | 0.1973(4) | 0.1963(5) | 0.2035(2) | 0.2027(6) | 0.2022(4) |
| | $U_{iso}$ | 0.005(1) | 0.006(1) | 0.008(1) | 0.006(1) | 0.008(1) | 0.005(1) | 0.007(1) |
| O3A | *x* | 0.1823(1) | 0.1824(2) | 0.1822(2) | 0.1822(2) | 0.1820(1) | 0.1822(2) | 0.1822(2) |
| | *y* | 1/4 | 1/4 | 1/4 | 1/4 | 1/4 | 1/4 | 1/4 |
| | *z* | 0.5539(3) | 0.5542(5) | 0.5530(6) | 0.5544(9) | 0.5558(3) | 0.5555(8) | 0.5557(5) |
| | $U_{eq}$ | 0.007(1) | 0.008(1) | 0.009(1) | 0.008(1) | 0.009(1) | 0.007(1) | 0.010(1) |
| O3B | *x* | 0.0685(1) | 0.0685(2) | 0.0689(2) | 0.0686(3) | 0.0687(1) | 0.0688(2) | 0.0688(2) |
| | *y* | 1/4 | 1/4 | 1/4 | 1/4 | 1/4 | 1/4 | 1/4 |
| | *z* | 0.2361(3) | 0.2355(5) | 0.2350(6) | 0.2358(9) | 0.2345(3) | 0.2350(8) | 0.2337(5) |
| | $U_{eq}$ | 0.007(1) | 0.008(1) | 0.009(1) | 0.009(1) | 0.009(1) | 0.007(1) | 0.009(1) |
| O4A | *x* | 0.3129(1) | 0.3127(1) | 0.3126(1) | 0.3122(2) | 0.3118(1) | 0.3117(2) | 0.3117(1) |
| | *y* | −0.0040(1) | −0.0045(1) | −0.0042(1) | −0.0046(2) | −0.0038(1) | −0.0039(2) | −0.0038(1) |
| | *z* | 0.5635(2) | 0.5616(4) | 0.5618(4) | 0.5627(6) | 0.5647(2) | 0.5648(6) | 0.5636(4) |
| | $U_{eq}$ | 0.007(1) | 0.007(1) | 0.010(1) | 0.008(1) | 0.010(1) | 0.008(1) | 0.008(1) |
| O4B | *x* | −0.0650(1) | −0.0649(1) | −0.0649(1) | −0.0651(2) | −0.0643(1) | −0.0643(2) | −0.0645(1) |
| | *y* | −0.0009(1) | −0.0012(1) | −0.0014(1) | −0.0008(2) | −0.0007(1) | −0.0004(2) | −0.0007(1) |
| | *z* | 0.2677(2) | 0.2673(4) | 0.2680(4) | 0.2677(6) | 0.2703(2) | 0.2704(6) | 0.2697(4) |
| | $U_{eq}$ | 0.007(1) | 0.008(1) | 0.009(1) | 0.0007(1) | 0.010(1) | 0.007(1) | 0.009(1) |
| O5A | *x* | 0.3055(1) | 0.3056(1) | 0.3056(1) | 0.3056(2) | 0.3049(1) | 0.3050(2) | 0.3048(1) |
| | *y* | 0.1152(1) | 0.1147(1) | 0.1147(1) | 0.1148(2) | 0.1157(1) | 0.1160(2) | 0.1158(1) |
| | *z* | −0.1641(2) | −0.1646(4) | −0.1646(4) | −0.1646(6) | −0.1659(2) | −0.1667(6) | −0.1657(4) |
| | $U_{eq}$ | 0.007(1) | 0.008(1) | 0.009(1) | 0.008(1) | 0.010(1) | 0.007(1) | 0.008(1) |
| O5B | *x* | −0.0544(1) | −0.0546(1) | −0.0543(1) | −0.0540(2) | −0.0537(1) | −0.0536(2) | −0.0537(1) |
| | *y* | 0.1139(1) | 0.1136(1) | 0.1135(1) | 0.1139(2) | 0.1136(1) | 0.1139(2) | 0.1134(1) |
| | *z* | 0.9511(2) | 0.9494(3) | 0.9488(4) | 0.9503(5) | 0.9512(2) | 0.9514(5) | 0.9517(4) |
| | $U_{eq}$ | 0.007(1) | 0.008(1) | 0.009(1) | 0.006(1) | 0.009(1) | 0.006(1) | 0.008(1) |
| O6A | *x* | 0.2966(1) | 0.2967(1) | 0.2967(1) | 0.2968(2) | 0.2975(1) | 0.2975(2) | 0.2974(1) |
| | *y* | 0.1297(1) | 0.1296(1) | 0.1300(1) | 0.1292(2) | 0.1294(1) | 0.1291(2) | 0.1295(1) |
| | *z* | 0.3364(2) | 0.3359(4) | 0.3371(5) | 0.3354(5) | 0.3345(2) | 0.3340(6) | 0.3342(4) |
| | $U_{eq}$ | 0.008(1) | 0.008(1) | 0.010(1) | 0.007(1) | 0.011(1) | 0.006(1) | 0.009(1) |
| O6B | *x* | −0.0464(1) | −0.0464(1) | −0.0463(1) | −0.0461(2) | −0.0468(1) | −0.0466(2) | −0.0466(1) |
| | *y* | 0.1333(1) | 0.1334(1) | 0.1330(1) | 0.1340(2) | 0.1340(1) | 0.1344(2) | 0.1337(1) |
| | *z* | 0.4507(2) | 0.4491(4) | 0.4487(4) | 0.4497(6) | 0.4513(2) | 0.4513(6) | 0.4517(4) |
| | $U_{eq}$ | 0.008(1) | 0.008(1) | 0.011(1) | 0.009(1) | 0.010(1) | 0.008(1) | 0.009(1) |
| O7A | *x* | 0.2930(1) | 0.2933(2) | 0.2931(2) | 0.2933(3) | 0.2948(1) | 0.2946(3) | 0.2946(2) |
| | *y* | 1/4 | 1/4 | 1/4 | 1/4 | 1/4 | 1/4 | 1/4 |
| | *z* | 0.0450(4) | 0.0425(6) | 0.0420(6) | 0.0429(9) | 0.0455(3) | 0.0447(9) | 0.0455(6) |
| | $U_{eq}$ | 0.009(1) | 0.009(1) | 0.010(1) | 0.009(1) | 0.011(1) | 0.009(1) | 0.011(1) |
| O7B | *x* | −0.0422(1) | −0.0426(2) | −0.0430(2) | −0.0430(3) | −0.0438(1) | −0.0441(2) | −0.0440(2) |
| | *y* | 1/4 | 1/4 | 1/4 | 1/4 | 1/4 | 1/4 | 1/4 |
| | *z* | 0.7556(3) | 0.7565(6) | 0.7561(6) | 0.7568(9) | 0.7595(3) | 0.7593(9) | 0.7597(5) |
| | $U_{eq}$ | 0.008(1) | 0.010(1) | 0.011(1) | 0.010(1) | 0.011(1) | 0.008(1) | 0.009(1) |

*Note:* $U_{eq}$ is defined as one third of the trace of the orthogonalized $U_{ij}$ tensor.

### Ferroholmquistite from Greenbushes, Western Australia

**Occurrence.** The Greenbushes lithian pegmatites (33° 45' S, 116° 5' E) occurs in the southwest part of Western Australia, 220 km south of Perth. The Greenbushes zoned pegmatite is one of the world's largest producers of tantalum and lithium, although it was first mined for alluvial tin. A large pegmatite body and several smaller ones intrude the Archaean Balingup Complex. The main body has sharply bounded Li-rich, K-rich, and Na-rich zones, the Na-rich zone being in the core. A review of the geology, mineralization, and geochronology of the Greenbushes pegmatite can be found in Partington et al. (1995) and references therein. Spodumene is the main lithium-bearing mineral phase, the others being amblygonite, holmquistite, and triphylite. Holmquistite and ferroholmquistite mainly occurs in the contact zones between amphibolites and intrusive dolerite, whereas the pegmatite is enriched in spodumene (Frost et al. 1987).

**Associated minerals.** These include albite, quartz, biotite, tourmaline, garnet, tin with tantalite inclusions, zircon, and scapolite (Partington et al. 1995). Holmquistites formed because of lithium migration from the pegmatite into the amphibolite (Frost et al. 1987). They belong to a late stage, and replace hornblende.

**Appearance, physical, and optical properties.** Ferroholmquistite occurs as elongated black to bluish-violet prismatic crystals, whose size is typically in the range 0.2–0.5 mm. It is translucent, with a vitreous luster, has a light bluish-violet

**TABLE 2B.** Atom coordinates, displacement parameters ($U_{iso}$, Å$^2$), and site-scattering values (s.s. in electrons per site) for the cationic sites

| Atom | | 1 | 2 | 3 | 4 | 5 | 6 | 7 |
|---|---|---|---|---|---|---|---|---|
| T1A | *x* | 0.2694(1) | 0.2695(1) | 0.2696(1) | 0.2695(1) | 0.2698(1) | 0.2697(1) | 0.2698(1) |
| | *y* | 0.1620(1) | 0.1620(1) | 0.1619(1) | 0.1622(1) | 0.1626(1) | 0.1626(1) | 0.1626(1) |
| | *z* | 0.0682(1) | 0.0673(1) | 0.0674(2) | 0.0677(2) | 0.0676(1) | 0.0676(2) | 0.0675(2) |
| | $U_{eq}$ | 0.004(1) | 0.004(1) | 0.006(1) | 0.004(1) | 0.006(1) | 0.004(1) | 0.005(1) |
| T1B | *x* | –0.0188(1) | –0.0188(1) | –0.0191(1) | –0.0188(1) | –0.0192(1) | –0.0190(1) | –0.0192(1) |
| | *y* | 0.1625(1) | 0.1624(1) | 0.1624(1) | 0.1626(1) | 0.1630(1) | 0.1631(1) | 0.1629(1) |
| | *z* | 0.7239(1) | 0.7232(1) | 0.7231(2) | 0.7238(2) | 0.7246(1) | 0.7247(2) | 0.7243(2) |
| | $U_{eq}$ | 0.004(1) | 0.005(1) | 0.006(1) | 0.004(1) | 0.006(1) | 0.004(1) | 0.005(1) |
| T2A | *x* | 0.2736(1) | 0.2736(1) | 0.2735(1) | 0.2736(1) | 0.2733(1) | 0.2733(1) | 0.2733(1) |
| | *y* | 0.0761(1) | 0.0759(1) | 0.0759(1) | 0.0762(1) | 0.0767(1) | 0.0767(1) | 0.0767(1) |
| | *z* | 0.5745(1) | 0.5733(1) | 0.5736(2) | 0.5734(2) | 0.5726(1) | 0.5727(2) | 0.5725(2) |
| | $U_{eq}$ | 0.004(1) | 0.004(1) | 0.006(1) | 0.004(1) | 0.006(1) | 0.004(1) | 0.005(1) |
| T2B | *x* | –0.0242(1) | –0.0242(1) | –0.0242(1) | –0.0243(1) | –0.0240(1) | –0.0241(1) | –0.0241(1) |
| | *y* | 0.0772(1) | 0.0770(1) | 0.0770(1) | 0.0773(1) | 0.0777(1) | 0.0779(1) | 0.0777(1) |
| | *z* | 0.2153(1) | 0.2145(1) | 0.2144(2) | 0.2153(2) | 0.2177(1) | 0.2176(2) | 0.2174(2) |
| | $U_{eq}$ | 0.004(1) | 0.005(1) | 0.006(1) | 0.005(1) | 0.006(1) | 0.004(1) | 0.005(1) |
| M1 | *x* | 0.1252(1) | 0.1252(1) | 0.1252(1) | 0.1252(1) | 0.1252(1) | 0.1252(1) | 0.1253(1) |
| | *y* | 0.1586(1) | 0.1589(1) | 0.1589(1) | 0.1590(1) | 0.1600(1) | 0.1600(1) | 0.1601(1) |
| | *z* | 0.3950(1) | 0.3947(1) | 0.3943(2) | 0.3948(2) | 0.3950(1) | 0.3949(2) | 0.3952(2) |
| | $U_{eq}$ | 0.006(1) | 0.007(1) | 0.007(1) | 0.007(1) | 0.006(1) | 0.006(1) | 0.006(1) |
| | *s.s.* | 18.91(5) | 16.99(8) | 16.77(6) | 16.34(10) | 14.88(4) | 14.62(11) | 14.55(4) |
| M2 | *x* | 0.1254(1) | 0.1254(1) | 0.1253(1) | 0.1253(1) | 0.1254(1) | 0.1253(1) | 0.1253(1) |
| | *y* | 0.0682(1) | 0.0687(1) | 0.0688(1) | 0.0685(1) | 0.0686(1) | 0.0685(1) | 0.0686(1) |
| | *z* | –0.1036(1) | –0.1039(1) | –0.1041(2) | –0.1038(2) | –0.1040(1) | –0.1043(2) | –0.1040(1) |
| | $U_{eq}$ | 0.005(1) | 0.005(1) | 0.007(1) | 0.005(1) | 0.006(1) | 0.003(1) | 0.005(1) |
| | *s.s.* | 14.36(4) | 13.64(7) | 13.60(5) | 14.54(9) | 17.75(4) | 17.87(11) | 17.59(4) |
| M3 | *x* | 0.1253(1) | 0.1253(1) | 0.1253(1) | 0.1254(1) | 0.1253(1) | 0.1254(1) | 0.1252(1) |
| | *y* | 1/4 | 1/4 | 1/4 | 1/4 | 1/4 | 1/4 | 1/4 |
| | *z* | –0.1052(1) | –0.1055(2) | –0.1060(2) | –0.1051(3) | –0.1051(1) | –0.1050(3) | –0.1053(2) |
| | $U_{eq}$ | 0.005(1) | 0.006(1) | 0.007(1) | 0.006(1) | 0.006(1) | 0.005(1) | 0.006(1) |
| | *s.s.* | 20.63(3) | 18.54(5) | 18.39(4) | 17.78(7) | 15.31(3) | 14.80(8) | 14.65(3) |
| M4 | *x* | 0.1233(2) | 0.1227(3) | 0.1239(4) | 0.1225(6) | 0.1241(2) | 0.1232(5) | 0.1235(3) |
| | *y* | –0.0088(2) | –0.0086(3) | –0.0091(3) | –0.0063(5) | –0.0069(2) | –0.0058(5) | –0.0075(2) |
| | *z* | 0.3981(6) | 0.3954(10) | 0.3986(12) | 0.3960(19) | 0.3979(6) | 0.3978(17) | 0.3962(12) |
| | $U_{eq}$ | 0.018(1) | 0.020(2) | 0.018(2) | 0.021(3) | 0.017(1) | 0.013(2) | 0.017(1) |
| | *s.s.* | 3.39(4) | 3.41(7) | 3.29(5) | 3.16(10) | 3.16(4) | 3.00(11) | 3.00(4) |
| HA | *x* | 0.2299 | 0.2312 | 0.2330 | 0.2353 | 0.2370 | 0.2375 | 0.2346 |
| | *y* | 1/4 | 1/4 | 1/4 | 1/4 | 1/4 | 1/4 | 1/4 |
| | *z* | 0.5542 | 0.5563 | 0.5446 | 0.5330 | 0.5680 | 0.5365 | 0.5481 |
| HB | *x* | 0.0141 | 0.0073 | 0.0221 | 0.0174 | 0.0150 | 0.0094 | 0.0188 |
| | *y* | 1/4 | 1/4 | 1/4 | 1/4 | 1/4 | 1/4 | 1/4 |
| | *z* | 0.2270 | 0.2307 | 0.2206 | 0.2492 | 0.2070 | 0.2355 | 0.2567 |

*Note:* $U_{eq}$ is defined as one third of the trace of the orthogonalized $U_{ij}$ tensor.

streak and Mohs hardness ~5–6, similar to all amphiboles. Ferroholmquistite is weakly pleochroic, with $\alpha$ = colorless, $\beta$ = pale violet-blue, and $\gamma$ = blue to deep violet. It is biaxial negative, with $\alpha$ = 1.628, $\beta$ = 1.646, and $\gamma$ = 1.651 ($\lambda$ = 589 nm). The calculated $2V_x$ angle based on the above refraction indexes is 55.1°. Orientation: **c** = *X*, with the optic axial plane coinciding with (010). The density calculated based on the unit formula and single-crystal unit-cell data is 3.145 g/cm$^3$.

**Chemical formula.** The formula resulting from combination of EMP, SIMS, and SREF analysis is: $^{A}(K_{0.01}Na_{0.01})^{B}(Li_{1.88}Mg_{0.08}Na_{0.03}Fe^{2+}_{0.01})^{C}(Al_{1.89}Fe^{2+}_{1.70}Mg_{1.39}Mn^{2+}_{0.02})^{T}Si_{8.00}O_{22}(OH_{1.97}F_{0.03})$; the simplified formula is: $^{A}\square^{B}Li_2{}^{C}(Fe^{2+}{}_3Al_2)^{T}Si_8O_{22}(OH)_2$, which requires: $Li_2O$ 3.53, FeO 25.48, $Al_2O_3$ 12.05, $SiO_2$ 56.81, $H_2O$ 2.13, total 100.00 wt%.

**X-ray powder analysis.** To fulfill the requirements of the IMA-CNMMN an XPRD pattern was recorded with a Philips PW1800 diffractometer using Cu*K*$\alpha$ radiation. Table 7 compares the experimental *d* values with those calculated based on the single-crystal refinement. Only the reflections compatible with the results of single-crystal analysis are reported in Table 7. Actually, the XPRD pattern was affected by several weak reflections resulting from the presence of inclusions, most of which were parawollastonite. The refined unit-cell parameters obtained from the *d*-values in the experimental powder pattern and least-squares fitting using the program Unit Cell by Holland and Redfern (1997) are: *a* = 18.279(8), *b* = 17.670(5), and *c* = 5.273(3) Å, and *V* = 1703.12 Å$^3$; they are in good agreement with those obtained from single-crystal analysis, i.e., *a* = 18.287(1), *b* = 17.680(1), and *c* = 5.278(1) Å, and *V* = 1706.45 Å$^3$.

## The crystal-chemistry of holmquistites

In the following discussion, all the structural data available for holmquistites and other orthorhombic amphiboles have been used together with the data of this work with the aim of monitoring crystal-chemical variations in holmquistites and ferroholmquistite.

## Site populations

Site populations were optimized by comparing the chemical composition obtained by EMP and SIMS analyses (Table 6) with the refined site-scattering values (Table 2) and mean bond-lengths (Table 3) under the constraint of overall electroneutrality. They are reported in Table 8, together with the disagreement parameters between the refined parameters and those calculated from the site populations. Highly charged cations are ordered at the M2 site, and their sum never exceeds 2.0 apfu.

**TABLE 3.** Selected bond-lengths (Å) and angles (°) for the holmquistite crystals of this work

| Sample | 1 | 2 | 3 | 4 | 5 | 6 | 7 |
|---|---|---|---|---|---|---|---|
| T1A-O1A | 1.632(1) | 1.634(2) | 1.633(3) | 1.631(3) | 1.632(1) | 1.626(3) | 1.630(2) |
| T1A-O5A | 1.620(1) | 1.621(2) | 1.621(3) | 1.624(3) | 1.619(1) | 1.620(3) | 1.616(2) |
| T1A-O6A | 1.606(1) | 1.606(2) | 1.609(3) | 1.607(3) | 1.608(1) | 1.608(3) | 1.606(2) |
| T1A-O7A | 1.619(1) | 1.618(1) | 1.618(1) | 1.615(2) | 1.617(1) | 1.617(2) | 1.616(1) |
| <T1A-OA> | 1.619 | 1.620 | 1.620 | 1.619 | 1.619 | 1.618 | 1.617 |
| TAV | 0.73 | 0.56 | 0.94 | 0.40 | 0.56 | 0.68 | 0.62 |
| TQE | 1.0002 | 1.0002 | 1.0002 | 1.0001 | 1.0002 | 1.0002 | 1.0002 |
| TILT | 5.10(1) | 5.05(2) | 5.12(2) | 5.05(2) | 4.15(1) | 4.29(2) | 4.19(2) |
| T1B-O1B | 1.631(1) | 1.632(2) | 1.631(3) | 1.631(3) | 1.630(1) | 1.625(3) | 1.632(2) |
| T1B-O5B | 1.613(1) | 1.610(2) | 1.606(3) | 1.606(3) | 1.611(1) | 1.609(3) | 1.614(2) |
| T1B-O6B | 1.613(1) | 1.614(2) | 1.617(3) | 1.610(3) | 1.612(1) | 1.610(3) | 1.609(2) |
| T1B-O7B | 1.614(1) | 1.616(1) | 1.616(1) | 1.615(2) | 1.615(1) | 1.615(2) | 1.618(2) |
| <T1B-OB> | 1.618 | 1.618 | 1.617 | 1.616 | 1.617 | 1.615 | 1.618 |
| TAV | 1.25 | 1.18 | 1.20 | 1.90 | 1.19 | 1.57 | 1.14 |
| TQE | 1.0003 | 1.0003 | 1.0003 | 1.0005 | 1.0003 | 1.0004 | 1.0003 |
| TILT | 4.92(1) | 4.85(2) | 4.64(2) | 4.53(2) | 4.04(1) | 3.94(2) | 3.97(1) |
| T2A-O2A | 1.633(1) | 1.634(2) | 1.632(3) | 1.631(3) | 1.628(1) | 1.625(3) | 1.630(2) |
| T2A-O4A | 1.589(1) | 1.590(2) | 1.585(2) | 1.593(3) | 1.590(1) | 1.591(3) | 1.590(2) |
| T2A-O5A | 1.650(1) | 1.650(2) | 1.650(3) | 1.648(3) | 1.648(1) | 1.646(3) | 1.649(2) |
| T2A-O6A | 1.629(1) | 1.626(2) | 1.628(3) | 1.622(3) | 1.626(1) | 1.625(3) | 1.627(2) |
| <T2A-OA> | 1.625 | 1.625 | 1.624 | 1.624 | 1.623 | 1.622 | 1.624 |
| TAV | 17.50 | 18.06 | 18.63 | 16.68 | 17.39 | 16.66 | 16.71 |
| TQE | 1.0043 | 1.0045 | 1.0046 | 1.0041 | 1.0043 | 1.0041 | 1.0041 |
| TILT | 8.94(2) | 8.76(3) | 8.72(4) | 8.58(5) | 7.84(2) | 7.82(4) | 7.83(3) |
| T2B-O2B | 1.635(1) | 1.637(2) | 1.637(3) | 1.638(3) | 1.636(1) | 1.629(3) | 1.636(2) |
| T2B-O4B | 1.594(1) | 1.593(2) | 1.596(2) | 1.592(3) | 1.596(1) | 1.594(3) | 1.597(2) |
| T2B-O5B | 1.634(1) | 1.637(2) | 1.638(3) | 1.633(3) | 1.636(1) | 1.634(3) | 1.630(2) |
| T2B-O6B | 1.641(1) | 1.639(2) | 1.634(3) | 1.640(3) | 1.639(1) | 1.640(3) | 1.637(2) |
| <T2B-OB> | 1.626 | 1.627 | 1.626 | 1.626 | 1.627 | 1.624 | 1.625 |
| TAV | 14.34 | 14.91 | 15.56 | 15.01 | 14.45 | 13.80 | 15.18 |
| TQE | 1.0035 | 1.0037 | 1.0039 | 1.0037 | 1.0036 | 1.0034 | 1.0038 |
| TILT | 9.19(2) | 9.14(3) | 9.20(4) | 9.21(5) | 8.44(2) | 8.56(5) | 8.63(3) |
| O5A-O6A-O5A | 166.9(1) | 166.6(1) | 166.4(1) | 167.0(2) | 168.0(1) | 168.3(2) | 168.0(1) |
| O5B-O6B-O5B | 163.9(1) | 163.6(1) | 163.9(1) | 163.5(2) | 163.5(1) | 163.4(2) | 163.5(1) |
| O7A-O7B | 4.766(3) | 4.760(4) | 4.765(4) | 4.753(6) | 4.712(3) | 4.714(6) | 4.711(3) |
| T1A-O7A-T1A | 147.8(1) | 147.4(2) | 147.7(3) | 147.3(3) | 146.0(1) | 146.0(3) | 146.2(2) |
| T1B-O7B-T1B | 146.9(1) | 146.2(2) | 146.2(3) | 145.8(3) | 144.9(1) | 144.3(3) | 144.6(2) |
| T1A-T2A | 3.017(1) | 3.017(1) | 3.017(1) | 3.018(2) | 3.023(1) | 3.021(2) | 3.022(1) |
| T1B-T2B | 3.002(1) | 2.999(1) | 3.001(1) | 3.000(2) | 3.009(1) | 3.007(2) | 3.008(1) |
| T1B-T1B | 3.094(1) | 3.092(1) | 3.092(2) | 3.086(2) | 3.079(1) | 3.075(2) | 3.082(2) |

*Notes:* TAV, TQE = tetrahedral angular variance and quadratic elongation; OAV, OQE = octahedral angular variance and quadratic elongation (Robinson et al. 1971).

Al and $Fe^{3+}$ disorder at the M1 and M3 sites in holmquistite had been suggested based on the agreement between observed and calculated octahedral distances (Irusteta and Whittaker 1975) and on the presence of minor bands shifted to slightly higher frequencies during IR (Law and Whittaker 1981) and Raman analysis (Kloprogge et al. 2001). In our opinion, the disagreement in the octahedral mean-bond lengths found by Irusteta and Whittaker (1975) was mainly due to the lack of correction for the F content, which reduces both the <M1-O> and the <M3-O> mean bond-lengths. The presence of minor bands in the OH-stretching region can now be better explained by the presence of very low amounts of Na substituting for Li at the M4 site. Iezzi et al. (2003) examined the ferri-clinoferroholmquistite–riebeckite join and found that the $Fe^{2+}$-$Fe^{2+}$-$Fe^{2+}$-$^{A}\square$-$^{M4}$Li-OH band occurs at 3614 $cm^{-1}$, whereas the $Fe^{2+}$-$Fe^{2+}$-$Fe^{2+}$-$^{A}\square$-$^{M4}$Na-OH band occurs at 3618 $cm^{-1}$. Law and Whittaker (1981) and Kloprogge et al. (2001) gave 3611 and 3614 $cm^{-1}$, respectively, for the $Fe^{2+}$-$Fe^{2+}$-$Fe^{2+}$-$^{A}\square$-$^{M4}$Li-OH band in holmquistite, and proposed a frequency shift of +7 $cm^{-1}$ for the minor bands, which were however poorly resolved. Ishida (1990) gave 3613 $cm^{-1}$ for the same band in ferroholmquistite from Greenbushes, and also found a very weak additional band at 3694 $cm^{-1}$, 65 $cm^{-1}$ from the Mg-$Fe^{2+}$-$Fe^{2+}$-$^{A}\square$-$^{M4}$Li-OH band, which was ascribed to the presence of A-site cations. More recently, Hawthorne et al. (1997) have shown that the shift from a vacant A-site environment induced by the presence of $^{A}$K is ~60 $cm^{-1}$, whereas that produced by $^{A}$Na is ~55 $cm^{-1}$.

### The M4 site

The M4 site is almost completely occupied by Li, but is also occupied by up to 0.08 Na apfu (crystal 6, Sweden) and up to 0.08 Mg apfu (crystal 1, W. Australia), showing that the charge arrangement in holmquistite is almost conservative. The shape of the electron density at the M4 site was carefully considered due to the high quality of the data. A small bump in the direction of the **b** edge was observed for sample 6 (with 0.08 Na apfu at the M4 site; Table 6), but a split position for Na was not inserted in the refined model. Out of the eight neighboring oxygen atoms, five are very close to the M4 cation (2.06–2.38 Å), two are within 2.73–2.95 Å, and one is beyond 3.47 Å. This coordination is rather unfortunate for Na, and this fact may explain the scarce solid-solution observed. This coordination is still suitable for Mg; constraints to Mg incorporation at the M4 sites should originate from the need to keep the octahedral strip small, i.e., of keeping the $R^{3+}$ content at the M2 site high.

### The octahedral sites

Refined site-scattering values and mean bond-lengths for all the investigated samples show that high-charged cations are

**TABLE 3.**—*CONTINUED*

| Sample | 1 | 2 | 3 | 4 | 5 | 6 | 7 |
|---|---|---|---|---|---|---|---|
| M1-O1A | 2.087(1) | 2.082(2) | 2.082(2) | 2.084(3) | 2.076(1) | 2.078(3) | 2.078(2) |
| M1-O1B | 2.084(1) | 2.080(2) | 2.081(2) | 2.082(3) | 2.077(1) | 2.077(3) | 2.076(2) |
| M1-O2A | 2.112(1) | 2.108(2) | 2.108(2) | 2.104(3) | 2.101(1) | 2.102(3) | 2.099(2) |
| M1-O2B | 2.123(1) | 2.123(2) | 2.118(2) | 2.126(3) | 2.112(1) | 2.120(3) | 2.118(2) |
| M1-O3A | 2.099(1) | 2.094(2) | 2.091(2) | 2.092(3) | 2.083(1) | 2.085(3) | 2.082(2) |
| M1-O3B | 2.095(1) | 2.089(2) | 2.086(2) | 2.087(3) | 2.080(1) | 2.078(3) | 2.081(2) |
| <M1-O> | 2.100 | 2.096 | 2.094 | 2.096 | 2.088 | 2.090 | 2.089 |
| OAV | 70.11 | 70.02 | 69.41 | 69.58 | 59.64 | 58.13 | 59.77 |
| OQE | 1.0211 | 1.0211 | 1.0209 | 1.0210 | 1.0180 | 1.0175 | 1.0180 |
| M2-O1A | 2.018(1) | 2.014(2) | 2.014(2) | 2.024(3) | 2.058(1) | 2.066(3) | 2.061(2) |
| M2-O1B | 2.020(1) | 2.014(2) | 2.022(3) | 2.020(3) | 2.061(1) | 2.059(3) | 2.057(2) |
| M2-O2A | 1.932(1) | 1.931(2) | 1.934(3) | 1.938(3) | 1.959(1) | 1.961(3) | 1.960(2) |
| M2-O2B | 1.941(1) | 1.933(2) | 1.937(3) | 1.931(3) | 1.967(1) | 1.969(3) | 1.962(2) |
| M2-O4A | 1.827(1) | 1.824(2) | 1.832(3) | 1.830 (3) | 1.853(1) | 1.854(3) | 1.852(2) |
| M2-O4B | 1.840(1) | 1.840(2) | 1.839(3) | 1.840(3) | 1.862(1) | 1.863(3) | 1.858(2) |
| <M2-O> | 1.930 | 1.926 | 1.930 | 1.931 | 1.960 | 1.962 | 1.958 |
| OAV | 30.96 | 29.99 | 29.86 | 31.53 | 34.86 | 34.35 | 34.31 |
| OQE | 1.0102 | 1.0099 | 1.0099 | 1.0105 | 1.0116 | 1.0115 | 1.0115 |
| M3-O1A x2 | 2.110(1) | 2.102(2) | 2.108(2) | 2.098(3) | 2.092(1) | 2.088(3) | 2.092(2) |
| M3-O1B x2 | 2.118(1) | 2.112(2) | 2.111(2) | 2.108(3) | 2.096(1) | 2.100(3) | 2.094(2) |
| M3-O3A | 2.080(2) | 2.076(3) | 2.079(4) | 2.074(5) | 2.069(2) | 2.072(5) | 2.071(3) |
| M3-O3B | 2.080(2) | 2.076(3) | 2.074(4) | 2.076(5) | 2.071(2) | 2.072(5) | 2.066(3) |
| <M3-O> | 2.102 | 2.097 | 2.099 | 2.094 | 2.086 | 2.087 | 2.085 |
| OAV | 94.93 | 92.96 | 90.66 | 90.83 | 75.3 | 74.19 | 75.32 |
| OQE | 1.0293 | 1.0287 | 1.0281 | 1.0280 | 1.0233 | 1.0229 | 1.0232 |
| M4-O2A | 2.125(4) | 2.133(6) | 2.119(6) | 2.109(11) | 2.100(4) | 2.096(10) | 2.116(6) |
| M4-O2B | 2.101(4) | 2.088(6) | 2.115(6) | 2.063(9) | 2.088(3) | 2.071(9) | 2.091(6) |
| M4-O4A | 2.129(4) | 2.132(6) | 2.136(7) | 2.133(10) | 2.123(3) | 2.130(9) | 2.129(6) |
| M4-O4B | 2.068(4) | 2.076(6) | 2.073(7) | 2.064(10) | 2.070(3) | 2.059(9) | 2.073(6) |
| M4-O5A | 2.311(4) | 2.307(6) | 2.290(6) | 2.345(9) | 2.348(4) | 2.377(9) | 2.347(5) |
| M4-O5B | 2.905(4) | 2.879(6) | 2.894(6) | 2.918(11) | 2.937(4) | 2.946(10) | 2.918(6) |
| M4-O6A | 3.474(4) | 3.483(6) | 3.466(7) | 3.496(11) | 3.475(5) | 3.488(10) | 3.479(7) |
| M4-O6B | 2.731(4) | 2.733(6) | 2.728(6) | 2.774(10) | 2.775(4) | 2.790(9) | 2.760(6) |
| $^{[VI]}$<M4-O> | 2.244 | 2.245 | 2.243 | 2.248 | 2.251 | 2.254 | 2.252 |
| HA-O3A | 0.87 | 0.89 | 0.93 | 0.98 | 1.01 | 1.02 | 0.96 |
| HB-O3B | 1.00 | 1.12 | 0.86 | 0.94 | 1.00 | 1.09 | 0.93 |
| M1-M4 | 2.960(4) | 2.957(6) | 2.965(5) | 2.919(9) | 2.953(4) | 2.934(9) | 2.966(4) |
| M2-M4 | 2.962(3) | 2.966(5) | 2.964(6) | 2.951(10) | 2.948(3) | 2.937(9) | 2.961(6) |
| T2A-M4 | 2.809(3) | 2.809(5) | 2.802(6) | 2.833(9) | 2.830(3) | 2.849(8) | 2.828(6) |

*Notes:* TAV, TQE = tetrahedral angular variance and quadratic elongation; OAV, OQE = octahedral angular variance and quadratic elongation (Robinson et al. 1971).

ordered at the M2 site. Al is the dominant high-charge constituent, $Fe^{3+}$ being significant only in Mg-richer samples, and Cr and Ti is always negligible. Similar to monoclinic amphiboles, $Fe^{2+}$ is preferentially ordered at the M3 site. It is interesting to note that the samples with the highest $Fe^{3+}$ contents (and thus with the largest M2 sites) are poor in $Fe^{2+}$ (and thus have small M1 and M3 sites). There seems to be a structural limit, which makes the overall dimension of the octahedral strip rather conservative.

The M1 and the M3 sites are strongly distorted, both in terms of octahedral angular variance (OAV) and of octahedral quadratic elongation (OQE) (Table 3). Distortion increases as a function of the $Fe^{2+}$ content, and tends to keep the octahedral volume constant.

As opposed to the monoclinic amphiboles, where there is extensive solid solution from the ferro- and ferri-ferro species of pedrizite toward clinoholmquistite, $^{C}$Li has never been detected in orthorhombic holmquistites. In monoclinic amphiboles, the occurrence of Li at the M3 site is associated with the charge arrangement of eckermannite [$^{A}R^{+}\,{}^{B}R_2^{+}\,{}^{C}(R_4^{2+}\,R_1^{3+})\,{}^{T}R_8^{4+}\,O_{22}\,{}^{W}R_2^{-}$] via the exchange vector $^{M2}R_1^{3+}\,{}^{M3}R_1^{+}\,{}^{M2,3}R_{-2}^{2+}$, and with the presence of Na or K at the A site to achieve a better charge balance for the oxygen atoms (Oberti et al. 2003a). The absence of A cations in holmquistites is thus coherent with the complete ordering of Li at the B sites. A very low A-site occupancy was however detected in crystal 6, where a small electron-density residual was found in the difference Fourier map at a very off-centered position equivalent to A*m* in monoclinic amphiboles [$x = 0.410$, $y = 1/2$, $z = 0.295$]. Its coordination is sixfold, but the A-O3B distance is too short (2.913 Å) to allow for the presence of an OH group at the neighboring O3B site. Were this maximum significant, the A-site occupancy should be locally associated with F at the O3B site (0.13 apfu in crystal 6). The refined M1-O3B bond-lengths are shorter than the M1-O3A bond-lengths (Table 3), which is also compatible with the ordering of F at the O3B site.

The M2-O4 bond-lengths are always very short (1.824–1.862 Å). This feature indicates that the O4 oxygen atom in the holmquistite structure is strongly underbonded, similarly to monoclinic amphiboles. Bond valence calculations were done for crystal 2 based on the results of this work and the parameters provided by Brese and O'Keeffe (1991) for the Si-O bonds and by Brown and Altermatt (1985) for the other bonds. They show that the incident bond-valence at the O4 sites is 1.876 valence units (v.u.) for the O4A site and 1.858 v.u. for the O4B site. Such low bond-valence values are known for leakeite A2 (1.856 v.u., Hawthorne et al. 1994), ferriwhittakerite (1.869 v.u., Oberti et al. 2004), fluoro-sodic-pedrizite (1.840 v.u., Oberti et al. 2005), where the M2-O4 distances are around 1.850 Å; they suggest a very stressed situation for the local environment of the O4A,B sites in holmquistites.

**TABLE 6.** Chemical analyses and mineral formulae (based on 24 O+F+Cl) for the holmquistite crystals of this work

| Sample | 1 | 2 | 3 | 4 | 5 | 6 | 7 | | 1 | 2 | 3 | 4 | 5 | 6 | 7 |
|---|---|---|---|---|---|---|---|---|---|---|---|---|---|---|---|
| No. pts | 5 | 6 | 4 | 5 | 8 | 6 | 8 | | | | | | | | |
| $SiO_2$ | 59.37 | 60.84 | 60.66 | 60.41 | 60.42 | 58.84 | 59.93 | Si | 8.00 | 7.99 | 7.97 | 8.00 | 8.00 | 8.00 | 8.00 |
| $TiO_2$ | 0.03 | 0.02 | 0.02 | 0.01 | 0.01 | 0.02 | 0.02 | Al | 0.00 | 0.01 | 0.03 | 0.00 | 0.00 | 0.00 | 0.00 |
| $Al_2O_3$ | 11.86 | 12.70 | 12.79 | 11.26 | 8.54 | 8.21 | 8.42 | Σ T | 8.00 | 8.00 | 8.00 | 8.00 | 8.00 | 8.00 | 8.00 |
| $Cr_2O_3$ | 0.00 | 0.01 | 0.00 | 0.01 | 0.03 | 0.01 | 0.02 | Al | 1.88 | 1.96 | 1.96 | 1.76 | 1.34 | 1.30 | 1.33 |
| MgO | 7.32 | 9.21 | 9.62 | 10.16 | 11.90 | 11.66 | 12.16 | Mg | 1.47 | 1.80 | 1.89 | 2.01 | 2.35 | 2.32 | 2.42 |
| CaO | 0.03 | 0.02 | 0.03 | 0.01 | 0.03 | 0.03 | 0.02 | $Fe^{2+}$ | 1.71 | 1.23 | 1.20 | 1.00 | 0.66 | 0.62 | 0.72 |
| MnO | 0.18 | 0.15 | 0.11 | 0.39 | 0.38 | 0.49 | 0.36 | $Fe^{3+}$ | 0.00 | 0.00 | 0.00 | 0.20 | 0.60 | 0.68 | 0.54 |
| $Fe_2O_3$ | 0.00 | 0.00 | 0.00 | 1.97 | 6.05 | 6.72 | 5.83 | $Mn^{2+}$ | 0.02 | 0.02 | 0.01 | 0.04 | 0.04 | 0.06 | 0.04 |
| FeO | 15.14 | 11.20 | 10.90 | 9.03 | 5.92 | 5.56 | 6.06 | $Zn^{2+}$ | 0.00 | 0.01 | 0.00 | 0.01 | 0.01 | 0.01 | 0.01 |
| ZnO | 0.02 | 0.06 | 0.01 | 0.09 | 0.14 | 0.14 | 0.14 | Li | 0.00 | 0.00 | 0.00 | 0.00 | 0.00 | 0.01 | 0.00 |
| $Na_2O$ | 0.17 | 0.11 | 0.13 | 0.11 | 0.21 | 0.37 | 0.21 | Σ C | 5.00 | 5.00 | 5.00 | 5.00 | 5.00 | 5.00 | 5.00 |
| $K_2O$ | 0.03 | 0.01 | 0.01 | 0.01 | 0.02 | 0.02 | 0.01 | Mg | 0.08 | 0.02 | 0.06 | 0.02 | 0.00 | 0.00 | 0.06 |
| F | 0.07 | 0.07 | 0.05 | 0.16 | 0.21 | 0.40 | 0.23 | Li | 1.88 | 1.98 | 1.91 | 1.97 | 1.98 | 1.92 | 1.93 |
| Cl | 0.01 | 0.00 | 0.00 | 0.00 | 0.01 | 0.01 | 0.01 | Na | 0.04 | 0.00 | 0.03 | 0.01 | 0.02 | 0.08 | 0.01 |
| $Li_2O_{SIMS}$ | 3.46 | 3.74 | 3.61 | 3.69 | * 3.71 | 3.58 | 3.59 | Σ B | 2.00 | 2.00 | 2.00 | 2.00 | 2.00 | 2.00 | 2.00 |
| $H_2O$* | 2.19 | 2.25 | 2.26 | 2.19 | 2.16 | 2.10 | 2.13 | Na | 0.00 | 0.03 | 0.00 | 0.02 | 0.03 | 0.02 | 0.04 |
| Sum | 99.88 | 100.36 | 100.20 | 99.34 | 99.68 | 98.06 | 99.08 | K | 0.01 | 0.00 | 0.00 | 0.00 | 0.00 | 0.00 | 0.00 |
| O=F,Cl | –0.03 | –0.03 | –0.02 | –0.07 | –0.09 | –0.13 | –0.10 | Σ A | 0.01 | 0.03 | 0.00 | 0.02 | 0.03 | 0.02 | 0.04 |
| Total | 99.85 | 100.33 | 100.18 | 99.27 | 99.59 | 97.93 | 98.98 | F | 0.03 | 0.03 | 0.02 | 0.07 | 0.09 | 0.13 | 0.10 |
| | | | | | | | | OH | 1.97 | 1.97 | 1.98 | 1.93 | 1.91 | 1.87 | 1.90 |
| *X* $Fe^{2+}$ | 0.52 | 0.40 | 0.38 | 0.33 | 0.22 | 0.21 | 0.23 | Σ O3 | 2.00 | 2.00 | 2.00 | 2.00 | 2.00 | 2.00 | 2.00 |
| *X* $Fe^{3+}$ | 0.00 | 0.00 | 0.00 | 0.16 | 0.48 | 0.52 | 0.43 | $ss_{cal}$† at C | 87.0 | 79.9 | 79.6 | 79.5 | 79.7 | 80.4 | 80.4 |
| Σ $R^{3+}$ | 1.88 | 1.96 | 1.96 | 1.96 | 1.94 | 1.98 | 1.87 | $ss_{cal}$ at B | 7.0 | 6.2 | 6.8 | 6.3 | 6.2 | 6.6 | 6.6 |
| | | | | | | | | $ss_{cal}$ at A | 0.2 | 0.3 | 0.0 | 0.2 | 0.3 | 0.2 | 0.4 |

* Calculated by stoichiometry.
† Site scattering calculated from the unit formulae (electrons per formula unit).

**TABLE 7.** XPRD Cu*K*α pattern of ferroholmquistite

| $I_{(calc)}$ | $I_{(exp)}$ | 2 $\theta_{(calc)}$ | 2 $\theta_{(exp)}$ | $d_{(calc)}$ | $d_{(exp)}$ | *h* *k* *l* | $I_{(calc)}$ | $I_{(exp)}$ | 2 $\theta_{(calc)}$ | 2 $\theta_{(exp)}$ | $d_{(calc)}$ | $d_{(exp)}$ | *h* *k* *l* |
|---|---|---|---|---|---|---|---|---|---|---|---|---|---|
| **100** | 100 | **10.89** | 10.91 | **8.1217** | 8.1128 | **2 1 0** | 6 | | 39.34 | | 2.2904 | | 5 5 1 |
| 3 | | 18.20 | | 4.8748 | | 1 1 1 | 5 | 2 | 42.23 | 42.23 | 2.1402 | 2.1383 | 5 0 2 |
| 4 | | 20.06 | | 4.4258 | | 2 1 1 | 5 | | 42.55 | | 2.1247 | | 5 1 2 |
| **26** | 2 | **20.09** | 20.09 | **4.4199** | 4.4199 | **0 4 0** | 5 | | 42.98 | | 2.1044 | | 5 6 1 |
| 4 | | 20.19 | | 4.3989 | | 1 2 1 | 3 | 1 | 46.17 | 46.14 | 1.9660 | 1.9672 | 6 6 1 |
| | 1 | | 21.89 | | 4.0601 | 2 2 1 | 3 | | 46.52 | | 1.9522 | | 7 5 1 |
| 5 | | 23.14 | | 3.8440 | | 1 3 1 | 3 | | 50.57 | | 1.8048 | | 2 9 1 |
| **13** | 4 | **24.65** | 24.60 | **3.6121** | 3.6191 | 2 3 1 | 4 | | 51.70 | | 1.7680 | | 0 10 0 |
| 4 | | 27.04 | | 3.2979 | | 2 5 0 | 4 | | 57.82 | | 1.5946 | | 9 6 1 |
| 7 | | 27.72 | | 3.2186 | | 4 2 1 | 3 | | 58.05 | | 1.5888 | | 8 8 0 |
| 9 | 2 | 28.08 | 28.09 | 3.1777 | 3.1766 | 4 4 0 | 6 | 7 | 58.29 | 58.28 | 1.5830 | 1.5818 | 2 11 0 |
| **48** | 10 | **29.74** | 29.73 | 3.0036 | 3.0047 | **6 1 0** | **12** | | **58.60** | | **1.5752** | | **0 5 3** |
| | 3 | | 30.18 | | 2.9617 | 5 1 1 | 4 | | 62.29 | | 1.4904 | | 2 6 3 |
| **17** | | **32.00** | | **2.7969** | | **2 5 1** | 3 | | 62.29 | | 1.4906 | | 10 6 1 |
| 10 | 5 | 33.09 | 33.06 | 2.7072 | 2.7095 | 6 3 0 | 6 | | 63.10 | | 1.4733 | | 0 12 0 |
| **14** | 1 | **33.87** | 33.85 | **2.6464** | 2.6480 | **3 5 1** | 3 | | 64.55 | | 1.4437 | | 0 7 3 |
| 7 | | 35.22 | | 2.5478 | | 1 6 1 | 3 | | 65.67 | | 1.4217 | | 6 11 0 |
| **11** | | **35.40** | | **2.5357** | | **2 0 2** | 5 | | 67.02 | | 1.3963 | | 11 6 1 |
| 7 | 1 | 36.35 | 36.31 | 2.4715 | 2.4743 | 4 5 1 | 3 | | 74.48 | | 1.2739 | | 2 12 2 |
| 5 | | 37.12 | | 2.4219 | | 3 0 2 | 4 | | 99.02 | | 1.0137 | | 14 11 0 |

*Note:* Calc = calculated from single-crystal data; exp = experimental. The eight strongest reflections are in bold.

**TABLE 8.** Site populations calculated based on chemical analyses and refined mean bond-lengths and site-scattering values

1 $^{A}(Na_{0.01}K_{0.01})^{M4}(Li_{1.88}Mg_{0.08}Na_{0.03}Fe^{2+}_{0.01})^{M1}(Mg_{1.00}Fe^{2+}_{0.98}Mn^{2+}_{0.01})^{M2}(Al_{1.89}Fe^{2+}_{0.11})^{M3}(Fe^{2+}_{0.61}Mg_{0.39})^{T1}Si_4{}^{T2}Si_4O_{22}{}^{O3}(OH_{1.97}F_{0.03})$
$\Delta_{<M1\text{-}O>} = -0.002$; $\Delta_{<M2\text{-}O>} = -0.006$; $\Delta_{<M3\text{-}O>} = -0.004$; $\Delta ss_{M1} = -0.4\%$; $\Delta ss_{M2} = 4.5\%$; $\Delta ss_{M3} = 0.4\%$; $\Delta ss_{M4} = -6.1\%$

2 $^{A}(Na_{0.03})^{M4}(Li_{1.98}Fe^{2+}_{0.02})^{M1}(Mg_{1.26}Fe^{2+}_{0.72}Mn^{2+}_{0.02})^{M2}(Al_{1.96}Fe^{2+}_{0.03}Zn_{0.01})^{M3}(Mg_{0.54}Fe^{2+}_{0.46})^{T1}(Si_{3.99}Al_{0.01})^{T2}Si_4O_{22}{}^{O3}(OH_{1.97}F_{0.03})$
$\Delta_{<M1\text{-}O>} = 0.001$; $\Delta_{<M2\text{-}O>} = -0.003$; $\Delta_{<M3\text{-}O>} = -0.002$; $\Delta ss_{M1} = -1.1\%$; $\Delta ss_{M2} = 2.6\%$; $\Delta ss_{M3} = 0.5\%$; $\Delta ss_{M4} = 5.3\%$

3 $^{A}\Delta^{M4}(Li_{1.91}Mg_{0.05}Na_{0.03}Fe^{2+}_{0.01})^{M1}(Mg_{1.31}Fe^{2+}_{0.68}Mn^{2+}_{0.01})^{M2}(Al_{1.96}Fe^{2+}_{0.04})^{M3}(Mg_{0.53}Fe^{2+}_{0.47})^{T1}(Si_{3.98}Al_{0.02})^{T2}Si_4O_{22}{}^{O3}(OH_{1.98}F_{0.02})$
$\Delta_{<M1\text{-}O>} = 0.000$; $\Delta_{<M2\text{-}O>} = 0.001$; $\Delta_{<M3\text{-}O>} = -0.001$; $\Delta ss_{M1} = -0.3\%$; $\Delta ss_{M2} = 2.5\%$; $\Delta ss_{M3} = -0.4\%$; $\Delta ss_{M4} = -5.3\%$

4 $^{A}(Na_{0.02})^{M4}(Li_{1.97}Na_{0.01}Mg_{0.01}Fe^{2+}_{0.01})^{M1}(Mg_{1.36}Fe^{2+}_{0.60}Mn^{2+}_{0.04})^{M2}(Al_{1.76}Fe^{3+}_{0.20}Mg_{0.02}Fe^{2+}_{0.01}Zn_{0.01})^{M3}(Mg_{0.62}Fe^{2+}_{0.38})^{T1}Si_4{}^{T2}Si_4O_{22}{}^{O3}(OH_{1.93}F_{0.07})$
$\Delta_{<M1\text{-}O>} = 0.003$; $\Delta_{<M2\text{-}O>} = -0.007$; $\Delta_{<M3\text{-}O>} = -0.001$; $\Delta ss_{M1} = -0.7\%$; $\Delta ss_{M2} = 0.7\%$; $\Delta ss_{M3} = 2.6\%$; $\Delta ss_{M4} = -1.3\%$

5 $^{A}(Na_{0.03})^{M4}(Li_{1.98}Na_{0.02})^{M1}(Mg_{1.55}Fe^{2+}_{0.40}Mn^{2+}_{0.04}Zn_{0.01})^{M2}(Al_{1.34}Fe^{3+}_{0.60}Fe^{2+}_{0.06})^{M3}(Mg_{0.80}Fe^{2+}_{0.20})^{T1}Si_4{}^{T2}Si_4O_{22}{}^{O3}(OH_{1.91}F_{0.09})$
$\Delta_{<M1\text{-}O>} = 0.000$; $\Delta_{<M2\text{-}O>} = -0.001$; $\Delta_{<M3\text{-}O>} = 0.000$; $\Delta ss_{M1} = -4.5\%$; $\Delta ss_{M2} = 1.7\%$; $\Delta ss_{M3} = -1.0\%$; $\Delta ss_{M4} = -2.7\%$

6 $^{A}(Na_{0.02})^{M4}(Li_{1.92}Na_{0.08})^{M1}(Mg_{1.54}Fe^{2+}_{0.40}Mn^{2+}_{0.06})^{M2}(Al_{1.30}Fe^{3+}_{0.68}Fe^{2+}_{0.01}Zn_{0.01})^{M3}(Mg_{0.78}Fe^{2+}_{0.21}Li_{0.01})^{T1}Si_4{}^{T2}Si_4O_{22}{}^{O3}(OH_{1.87}F_{0.13})$
$\Delta_{<M1\text{-}O>} = 0.001$; $\Delta_{<M2\text{-}O>} = 0.001$; $\Delta_{<M3\text{-}O>} = 0.000$; $\Delta ss_{M1} = -3.9\%$; $\Delta ss_{M2} = 1.7\%$; $\Delta ss_{M3} = -0.3\%$; $\Delta ss_{M4} = -0.6\%$

7 $^{A}(Na_{0.04})^{M4}(Li_{1.93}Mg_{0.06}Na_{0.01})^{M1}(Mg_{1.53}Fe^{2+}_{0.43}Mn^{2+}_{0.04})^{M2}(Al_{1.33}Fe^{3+}_{0.54}Fe^{2+}_{0.11}Mg_{0.01}Zn_{0.01})^{M3}(Mg_{0.82}Fe^{2+}_{0.18})^{T1}Si_4{}^{T2}Si_4O_{22}{}^{O3}(OH_{1.90}F_{0.10})$
$\Delta_{<M1\text{-}O>} = 0.000$; $\Delta_{<M2\text{-}O>} = -0.007$; $\Delta_{<M3\text{-}O>} = 0.000$; $\Delta ss_{M1} = -4.0\%$; $\Delta ss_{M2} = 2.5\%$; $\Delta ss_{M3} = 5.2\%$; $\Delta ss_{M4} = -4.8\%$

*Note:* Δ = differences between the observed parameters and those calculated from the site populations.

### The tetrahedral sites

No significant Al substitution was detected in the investigated samples. The pattern of the mean bond-lengths is similar to that of monoclinic amphiboles, where the T1 site is smaller and more regular than the T2 site. Crystals 2 and 3, with <0.02 $^{T}$Al pfu, have the longest <T1A-OA> and <T1A-O> distances (Table 3). This data may suggest that $^{T}$Al orders at the T1 sites, similarly to monoclinic amphiboles, and might also further order at the T1A site in holmquistites.

The two independent double-chains of tetrahedra mainly differ in their conformation. Generally, the O5-O6-O5 angles (which are a measure of the stretching along the **c** axis) are greater in the A chain (166.4–168.3°) than in the B chain (163.4–163.9°). The T1-O7-T1 angles (which are a measure of the stretching along the **b** axis) are slightly but significantly larger in the A chain than in the B chain.

These data confirm the comment made by Irusteta and Whittaker (1975), who noted that the double chains of tetrahedra in holmquistite are more extended (especially the B chain) and have more similar conformation than in the other orthorhombic amphiboles. The stretching of the double chains of tetrahedra must be related to the relative sizes of the various structural moduli. Gedrite, ideally $Mg_2(Mg_3Al_2)(Si_6Al_2)O_{22}(OH)_2$, couples the largest tetrahedra with the smallest M1,2,3,4 polyhedra, and thus the two double-chains of tetrahedra are the most kinked (162.5 and 146.0°, respectively; Papike and Ross 1970). Anthophyllite, ideally $Mg_2Mg_5Si_8O_{22}(OH)_2$, couples the smallest tetrahedra with larger M2 sites, and the two chains are significantly more extended (169.2 and 157.5°, respectively, Finger 1970; 169.4 and 157.9°, respectively, Walitzi et al. 1989). Holmquistite, ideally $Li_2(Mg_3Al_2)Si_8O_{22}(OH)_2$, couples the smallest tetrahedra with the smallest octahedra, and with an M4 polyhedron only slightly larger than in the other two orthorhombic end-members. As a result, both the stretching and kinking angles are more relaxed. Notably, the kinking does not vary much in the holmquistites of this work, where the average dimensions of the octahedral strip are kept constant by the absence of $Fe^{3+}$ in $Fe^{2+}$-rich samples. The kinking of the A double chain is slightly greater in the $Fe^{2+}$-richer samples (Table 3).

### Geometrical constraints on the stability of holmquistites

The holmquistite structure is very compact. The presence of a small monovalent cation at the M4 site allows for very short M4-M1, M4-M2, and M4-T2 distances. Even more importantly, the small dimensions of the three independent octahedra, as well as the absence of $^{T}$Al, imply the shortest T1-T2 (short) distances ever found for amphiboles (down to 2.999 Å in crystal 2; Table 3). The other orthorhombic amphiboles have larger T1-T2 (short) values (3.048 in anthophyllite and 3.026 Å in gedrite), whereas Fe-poorest glaucophanes may reach 3.003 Å (CNR-IGG, unpublished). In the studied holmquistites, the shortest T1-T2 (short) distances occur in the $Fe^{2+}$, Al-richer crystals of this work, where the small but distorted M2 octahedron has a short O1B-OB2 edge. The O1-O2 edge is shared with the M1 octahedron, and thus the $Mg_{-1}Fe^{2+}_{1}$ substitution at the M1 site in principle acts against this mechanism. However, the M3 octahedron is strongly elongated along the **b** axis. The presence of a small monovalent cation at the M4 site, and the consequent underbonding of the O4 oxygen atom, however, constrain the M2-O4A,B distances; as a consequence, the M2 octahedron expands mainly along the [010] direction, pushes the M3 octahedron and thus limits the occupancy of $Fe^{2+}$ at this site. In $Fe^{3+}$-richer samples, the O1B-OB2 edge lengthens, and the O5A-O6A-O5A angles relax (e.g., crystals nos. 5, 6, and 7).

This structural limits does not exist in gedrites, where the presence of a small but divalent cation at the M4 site allows the heterovalent exchange $Si_{-1}Al$ at the T1 sites, and thus the expansion of the M1 and M3 octahedra along [010]. Accordingly, large $Fe^{2+}$ contents are commonly found in gedrites (cf. Deer et al. 1997 for a review).

### Unit-cell dimensions

All our data show that compositional and structural variations are limited in holmquistites, a feature that may be interpreted in terms of a narrow stability field for the orthorhombic structure in $^{B}$Li amphiboles. As a consequence, the unit-cell dimensions also show very limited variations; in particular, the *c* edge is virtually invariant. Relations between the length of the unit-cell edges and the crystal-chemical composition were carefully looked for. The interesting features are reported in Figure 1,

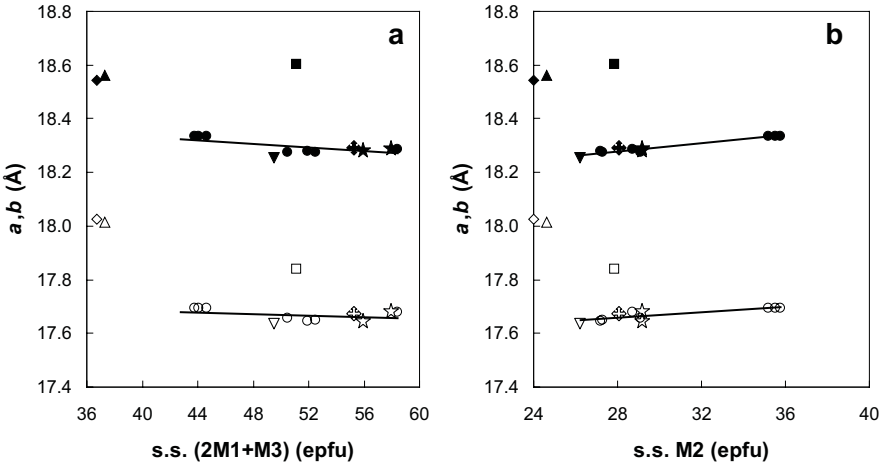


**FIGURE 1.** The *a* and *b* cell parameters vs. the total refined site scattering at the M1 and M3 sites (~$Fe^{2+}$ content) (a) and the refined site scattering at the M2 sites (~$Fe^{3+}$ content) in orthorhombic amphiboles. Full symbols = *a*-edge; empty symbols = *b*-edge. Dots = this work; arrow-cross = holmquistite (Irusteta and Whittaker 1975); star = holmquistite (Puvvada 1991); downward triangle = holmquistite (Walter et al. 1989); upward triangle = anthophyllite (Finger 1970); diamond = anthophyllite (Walitzi et al. 1989); square = gedrite, sample 002 (Papike and Ross 1970).

which compares all the data available in the literature for holmquistites, for a gedrite with 0.16 $Fe^{3+}$, 2.35 $Fe^{2+}$, and 0.50 $^{A}Na$ apfu (Papike and Ross 1970) and for two anthophyllite crystals close to the ideal $^{A}\square^{B}Mg_2{}^{C}Mg_5{}^{T}Si_8O_{22}(OH)_2$ formula. The comparison between gedrite and anthophyllite shows that the presence of (smaller) trivalent cations at the M2 site strongly shortens the *b* dimension, whereas that of the (larger) trivalent tetrahedral cation and/or Na at the A site lengthens the *a* edge**.** In holmquistites, the $Al_{-1}Fe^{3+}$ exchange at the M2 site slightly lengthens both the *a* and the *b* dimensions. On the contrary, the $Mg_{-1}Fe^{2+}$ exchange at the M1 and the M3 sites is not important, and the effect of the simultaneous $Fe^{3+}_{-1}Al$ exchange is prevailing and keeps the *b* edge short. This is a very unusual behavior in rock-forming mineral families, especially the amphiboles, where the unit-cell parameters are always good indicators of the overall compositional changes and of the distributions of some cations within the various sites.

### General remarks

All the evidences discussed above provide arguments for the non-existence of holmquistite samples with compositions close to those of the ferro-, ferri-, or ferri-ferro-end-members. Also, recent studies have shown that clinoholmquistite has never been found in nature (Oberti et al. 2005), and could not be synthesized under proper chemical and physico-chemical conditions (Iezzi et al. 2004). In this latter study, the presence of Fe was found to be essential to the stability of the monoclinic structure.

The situation of $^{B}Li$ amphiboles thus is similar to that of $^{B}Mg$ amphiboles, where orthorhombic anthophyllites have Mg/Fe values higher than 0.60, Mg-rich cummingtonites are very rare (and have $P2_1/m$ symmetry), but the Fe- and Mn-rich members of the cummingtonite-grunerite series are common (and have the standard $C2/m$ symmetry). On the contrary, gedrites cover the whole range of Mg/Fe ratios (cf. Deer et al. 1997 for a review). Also, partial-to-dominant Na occupancy at the A site is reported for anthophyllites (where it is balanced by Al at the T1 sites) and for gedrites (where it is balanced by less Al at the M2 site). On the contrary, significant $^{A}Na$ has never been reported for holmquistites but is common in ferro-, ferri-, and ferri-ferro-clinoholmquistites, where it couples with the presence of Li at the M3 site (thus giving rise to extensive solid-solution toward pedrizites).

We can conclude that the coexistence of a strip composed of the smallest possible octahedra with double chains composed of the smallest possible tetrahedra is favored in the orthorhombic symmetry, where the two double chains forming an I beam become symmetrically independent and may assume different conformations, which are both strongly kinked. In this symmetry, an irregular and lower coordination suitable for Li at the M4 site is provided. An enlargement of the octahedral strip that was not combined with $^{T}Al$ substitution would imply a further stretching of the double chains of tetrahedra, and would give rise to a transition to monoclinic symmetry.

## Acknowledgments

We thank the mineral collectors who kindly provided the holmquistite samples investigated during this work, in particular G. Pierini, P. Gorini (both from Varese, Italy) and R. and A. Pagano (Cinisello Balsamo, Milan, Italy), who provided the ferroholmquistite holotype. L. Ottolini (CNR-IGG Pavia) is warmly thanked for doing SIMS analysis for Li, and J. Gray (Department of Geology, Georgia State University, Atlanta) for measuring the optical properties of ferroholmquistite. M. Serracino (CNR-IGAG, Rome) and F. Bellatreccia (Dipartimento di Scienze della Terra, Università La Sapienza, Rome) provided EMP analyses.

## References cited

Blessing, R.H., Coppens, P., and Becker, P. (1974) Computer analysis of step scanned X-ray data. Journal of Applied Crystallography, 7, 488–492.

Brese, N.S. and O'Keeffe, M. (1991) Bond-valence parameters for solids. Acta Crystallographica, B47, 192–197.

Brown, I.D. and Altermatt, D. (1985) Bond-valence parameters obtained from a systematic analysis of the Inorganic Crystal Structure Database. Acta Crystallographica, B41, 244–247.

Deer, W.A., Howie, R.A., and Zussman, J. (1997) Rock forming minerals, vol. 2B, 2nd ed., Double-chain Silicates. The Geological Society, London.

Finger, L.W. (1970) Refinement of the crystal structure of an anthophyllite. Carnegie Institution Washington Year Book, 68, 283–288.

Frost, M.T., Tsambourakis, G., and Davis, J. (1987) Holmquistite-bearing amphibolite from Greenbushes, Western Australia. Mineralogical Magazine, 51, 585–591.

Ginzburg, I.V. (1965) Holmquistite and its structural variety clinoholmquistite. Trudy Mineralogicheskogo Muzeya Akademii Nauk SSSR, 16, 73–89.

Hawthorne, F.C., Ungaretti, L., Oberti, R., Cannillo, E., and Smelik, E.A. (1994) The mechanism of $^{[6]}Li$ incorporation in amphiboles. American Mineralogist, 79, 443–451.

Hawthorne, F.C., Della Ventura, G., Robert, J.L., Welch, M.D., Raudsepp, M., and Jenkins, D.M. (1997) A Rietveld and infrared study of synthetic amphiboles along the potassium-richterite-tremolite join. American Mineralogist, 82, 708–716.

Holland, T.J.B. and Redfern, S.A.T. (1997) Unit cell refinement from powder diffraction data: the use of regression diagnostics. Mineralogical Magazine, 61, 65–77.

Iezzi, G., Della Ventura, G., Cámara, F., Pedrazzi, G., and Robert, J.-L. (2003) $^{B}Na$-$^{B}Li$ solid solution in A-site vacant amphiboles: synthesis and cation ordering along the ferri-clinoferroholmquistite-riebeckite join. American Mineralogist, 88, 955–961.

Iezzi, G., Della Ventura, G., Cámara, F., Oberti, R., and Robert, J.-L. (2004) Li-bearing amphiboles: synthesis, stability and composition of clinoholmquistites. 32nd International Geological Congress, Florence, 20–28 August 2004, Abstracts.

Irusteta, M.C. and Whittaker, E.J.W. (1975) A three-dimensional refinement of the structure of holmquistite. Acta Crystallographica, B31, 145–150.

Ishida, K. (1990) Identification of infrared OH librational bands of talc-willemseite solid solution and $Al^{(IV)}$-free amphiboles through deuteration. Mineralogical Journal, 15, 93–104.

Khvostova, V.A. (1958) A new discovery of holmquistite. Doklady Akademii Nauk SSSR, 118, 1027–1030.

Kloprogge, J.T., Case, M.H., and Frost, R.L. (2001) Raman mocroscopic study of the Li amphibole holmquistite, from the Martin Marietta Quarry, Bessemer City, NC, USA. Mineralogical Magazine, 65, 775–783.

Knorring von, O. and Hornung, G. (1961) On the lithium amphibole holmquistite, from Benson pegmatite mine, Mtoko, Southern Rhodesia. Mineralogical Magazine, 32, 731–735.

Law, A.D. and Whittaker, E.J. (1981) Studies of the orthoamphiboles I—The Mössbauer and infrared spectra of holmquistite. Bulletin de Minéralogie, 104, 381–386.

Lehmann, M.S. and Larsen, F.K. (1974) A method for location of the peaks in step scan-measured Bragg reflections. Acta Crystallographica, A30, 580–584.

Litvin, A.L., Ginzburg, I.V., Egorova, L.N., and Ostapenko, S.S. (1973) On the crystal structure of holmquistite. Konstitutsiya i Svoystva Mineralov, 7, 18–31.

Litvin, A.L., Ginzburg, I.V., Egorova, L.N., and Petrunina, A.A. (1975) On the crystal structure of clinoholmquistite. Konstitutsiya i Svoystva Mineralov, 9, 3–6.

London, D. (1986) Holmquistite as a guide to pegmatitic rare metal deposits. Economic Geology, 81, 704–712.

North, A.C.T., Phillips, D.C., and Mathews, F.S. (1968) A semi-empirical method of absorption correction. Acta Crystallographica, A24, 351–359.

Oberti, R., Cámara, F., Ottolini, L., and Caballero, J.M. (2003a) Lithium in amphiboles: detection, quantification, and incorporation mechanisms in the compositional space bridging sodic and $^{B}Li$-amphiboles. European Journal of Mineralogy, 15, 309–319.

Oberti, R., Cámara, F., Caballero, J.M., and Ottolini, L. (2003b) Sodic-ferri-ferropedrizite and ferri-clinoferroholmquistite: mineral data and degree of order of the A-site cations in Li-rich amphiboles. Canadian Mineralogist, 41, 1345–1354.

Oberti, R., Cámara, F., and Caballero, J.M. (2004) Ferri-ottoliniite and ferriwhittakerite, two new end-members of the new Group 5 for monoclinic amphiboles. American Mineralogist, 89, 888–893.

Oberti, R., Cámara, F., and Ottolini, L. (2005) Clinoholmquistite discredited: the new amphibole end-member fluoro-sodic-pedrizite. American Mineralogist, 90, 732–736.

Ottolini, L. and Oberti, R. (2000) Accurate quantification of H, Li, Be, B, F, Ba, REE, Y, Th, and U in complex matrixes: a combined approach based on SIMS and single-crystal structure refinement. Analytical Chemistry, 72, 3731–3738.

Palache, C., Davidson, S.C., and Goranson, E.A. (1930) The hiddenite deposit in Alexander County, North Carolina. American Mineralogist, 15, 280–302.

Papike, J.J. and Ross, M. (1970) Gedrites: Crystal structures and intracrystalline cation distributions. American Mineralogist, 55, 1945–1972.

Partington, G.A., McNaughton, N.J., and Williams, I.S. (1995) A review of the geology, mineralisation and geochronology of the Greenbushes Pegmatite, Western Australia. Economic Geology, 90, 616–635.

Pouchou, J.L. and Pichoir, F. (1985) 'PAP' Φ(ρZ) procedure for improved quantitative micro-analysis. Microbeam Analysis, 104–160.

Puvvada, G.P. (1991) Crystal-chemistry of holmquistite. M.Sc. Thesis, Brigham Young University, Provo, Utah.

Robinson, K., Gibbs, G.V., and Ribbe, P.H. (1971) Quadratic elongation: A quantitative measure of distortion in coordination polyhedra. Science, 172, 567–570.

Sheldrick, G.M. (1996) SADABS, Siemens area detector absorption correction software. University of Goettingen, Germany.

——— (1997) SHELX-97. Programs for Crystal Structure Determination and Refinement. University of Goettingen, Germany.

Walitzi, E.M., Walter, F., and Ettinger, K. (1989) Verfeinerung der Kristallstruktur von Anthophyllite vom Ochsenkogel/Gleinalpe, Österreich. Zeitschrift für Kristallographie, 188, 237–244.

Walter, F., Walitzi, E.M., and Mereiter, K. (1989) Verfeinerung der Kristallstruktur von Holmquistit vom Brandrücken/Weienebene. Koralpe. Österreich. Zeitschrift für Kristallographie, 188, 95–101.

Whittaker, E.J.W. (1969) The structure of the orthorhombic amphibole holmquistite. Acta Crystallographica, B25, 394–397.

MANUSCRIPT RECEIVED AUGUST 18, 2004
MANUSCRIPT ACCEPTED OCTOBER 29, 2004
MANUSCRIPT HANDLED BY SIMONA QUARTIERI